LUND UNIVERSITY

Design of Energy Saving Windows with High Transmission at 900 MHz and 1800 MHz

Widenberg, Björn; Rodriguez, José Victor

2002

[Link to publication](#)

Design of Energy Saving Windows with High Transmission at 900 MHz and 1800 MHz

Björn Widenberg and José Víctor Rodríguez Rodríguez

Department of Electroscience
Electromagnetic Theory
Lund Institute of Technology
Sweden
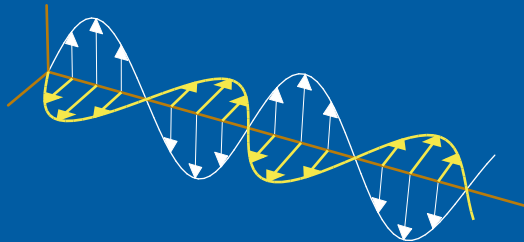
Björn Widenberg
José Víctor Rodríguez Rodríguez

Department of Electroscience
Electromagnetic Theory
Lund Institute of Technology
P.O. Box 118
SE-221 00 Lund
Sweden

Abstract

This paper focuses on the radio wave propagation through energy saving windows. These panes have a metallic shielding that keeps the heat inside the building during winter and outside during summer. Unfortunately, this covering also has an opaque behaviour at microwave frequencies. A design of energy saving window panes with high transmission at $900\,\mathrm{MHz}$ and $1800\,\mathrm{MHz}$ is presented. The high transmission is obtained by perforating the metallic shielding with narrow slits so that a Frequency Selective Structure (FSS) is formed. A parameter study of the resulting FSS is then considered.

1   Introduction

Transmission of microwave frequencies into indoor environments through windows should not be a problem, since glass has a very low conductivity (typically $\sigma = 10^{-12}\,\mathrm{S/m}$) and a moderate relative permittivity ($\epsilon_r = 5.5$), and since the panes are thin compared to the wavelength. However, in modern buildings this assumption is not true due to the fact that energy saving window panes are used, see Figure 1. These special panes have the finality of keeping the heat inside the indoor environment during winter and out of the building during summer. In order to get this property, the panes are covered with a very thin metallic shielding that prevents frequencies placed in the infrared from passing through the window, see Figure 2. The panes are transparent for the visible part of the electromagnetic spectrum.

It has been reported that this metallic shielding is opaque for microwaves [2, 5, 10, 14]. In Figure 3 transmission measurements at $1800\,\mathrm{MHz}$ for different glass plates are presented. The transmission curves were measured when no glass plate, a single glass plate, and a double glass plate with metallic shielding were present in the window frame. The transmission for the two first cases was very good, a window with no shielding has almost as good transmission as with no pane. When the second double glass plate was fitted an attenuation of -20dB can be observed. This was caused by the metal shielding. The drop is comparable to the one that takes place when the entire window gap is covered by a metal sheet. Thus, the full window (with metallic shielding) dramatically decreases the level of the transmitted signal, being pretty similar to the one received through a Perfectly Electric Conducting (PEC) plate [2]. The problem with energy saving windows is illustrated in Figure 2.

Both tin oxide (SnO) and silver (Ag) are used as both a thermal and optical reflector. The optical reflector is to prevent view from the outside through the window. The metallic layers are extremely thin (typically $4000\,\text{Å}$ for SnO, $100 - 200\,\text{Å}$ for Ag), and much thinner than the skin depth at UHF-frequencies ($20000\,\text{Å}$ for Ag at $1.0\,\mathrm{GHz}$). The reason for the low transmission is the near-perfect reflection at the interface of the metal layer.

The transmission from an outdoor base station to a mobile phone placed inside an indoor environment with energy saving window panes has to be through the walls. The deterioration of the radio link is compensated by the mobile phone by increasing its radiated power, which is unwanted. The problem of the opaque behaviour

Figure 1: Modern building with energy saving window panes.

of window energy panes at microwaves will be worse in the future, when communications are placed at higher frequencies, since it is known that the attenuation of waves propagating through walls increases with frequency [7].

In this paper, the design of energy saving window panes with high transmission at certain microwave frequencies (especially at 900 MHz and 1800 MHz) [16] without affecting the properties at infrared and visible light is discussed. The desired behaviour is reached by making very narrow slits ordered in a periodic pattern in the metallic shielding. Such a structure is called a Frequency Selective Structure (FSS) [8, 13, 17, 18]. The frequency behaviour of the FSSs depends on the shape of the slots and in this particular study, they are modelled as very narrow rectangles.

This paper shows one possible application to use Frequency Selective Structure (FSS) in radio communication, without doubt there are several more applications for these structures.

2   Frequency Selective Structures

Frequency Selective Structures (FSSs) are metal screens perforated periodically with apertures or dielectric screens with periodic arrays of metallic patches. They are used as filters in the microwave, the mm, and the sub-mm wave range. Two-dimensional planar periodic structures have attracted a great amount of attention because of their frequency filtering property, see Figure 4.

The frequency behaviour of the FSSs depends on the shape of the elements (apertures/patches), on their size and spacing, and on the thickness of the metal screen. Common element shapes are: circular, rectangular/dipole, crossed dipole, ring. Similar to the frequency filters in traditional Radio-Frequency (RF) circuits, the FSS may have low-pass or high-pass spectral behaviour, depending upon the array element type (patch or aperture, respectively) [18].
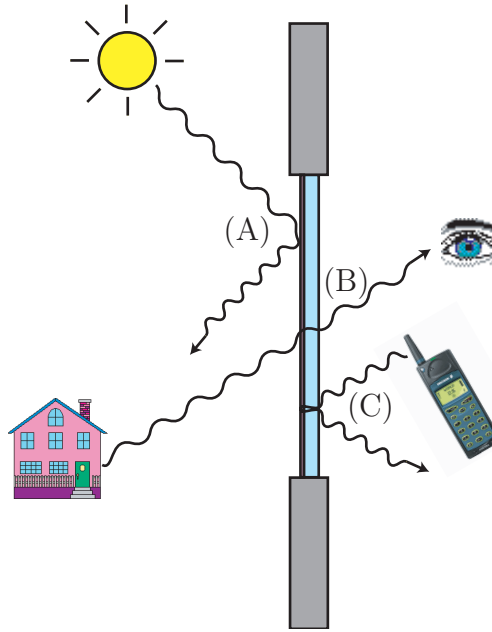
Figure 2: Illustration of the problem. The window pane has an opaque behaviour for heat, *i.e.*, IR-radiation (A), and is transparent for the visible part of the spectrum (B), but microwaves are also stopped (C), which is unwanted.

When a strip dipole element is illuminated by an RF source, and if the length of the dipole is a multiple of a half-wavelength, the dipole will resonate and scatter the energy. When many strip dipoles are arrayed (patches), the re-radiated energy from all the elements will be coherent toward the direction as if a reflection is occurring, when the reflection angle equals the angle of incidence. The reason is that the induced surface current on each strip has a phase delay relative to its neighboring element. It is this phase delay that causes the scattered waves from all the elements to be coherent. When the element size deviates from the resonant dimensions, the incident wave travels through an FSS screen as if the screen is almost transparent. A small loss will occur due to dielectric, metal conduction, and scattering [18].

The structure complementary to the dipole structure is the slot (or aperture) array, such that if the two complementary arrays are put on top of each other, a "complete" perfectly conducting plate is obtained. It can be shown that, for free-standing thin grids without dielectrics, the specular reflection coefficient for one array equals the transmission coefficient for the complementary array [8].

Dielectrics are often used as structural support. They also stabilize the drift of the FSSs resonant frequency with the steering of incident angle. The resonant frequencies decrease as the dielectric thickness increases. The FSSs also depend on the incident angle and the wave polarization, when a dielectric load is considered. Two basic dielectric configurations can be found: the grids are bonded on one side, and the grids are embedded centrally in the dielectrics. One of the most important applications of dielectric loading is the multiband FSS design [19].
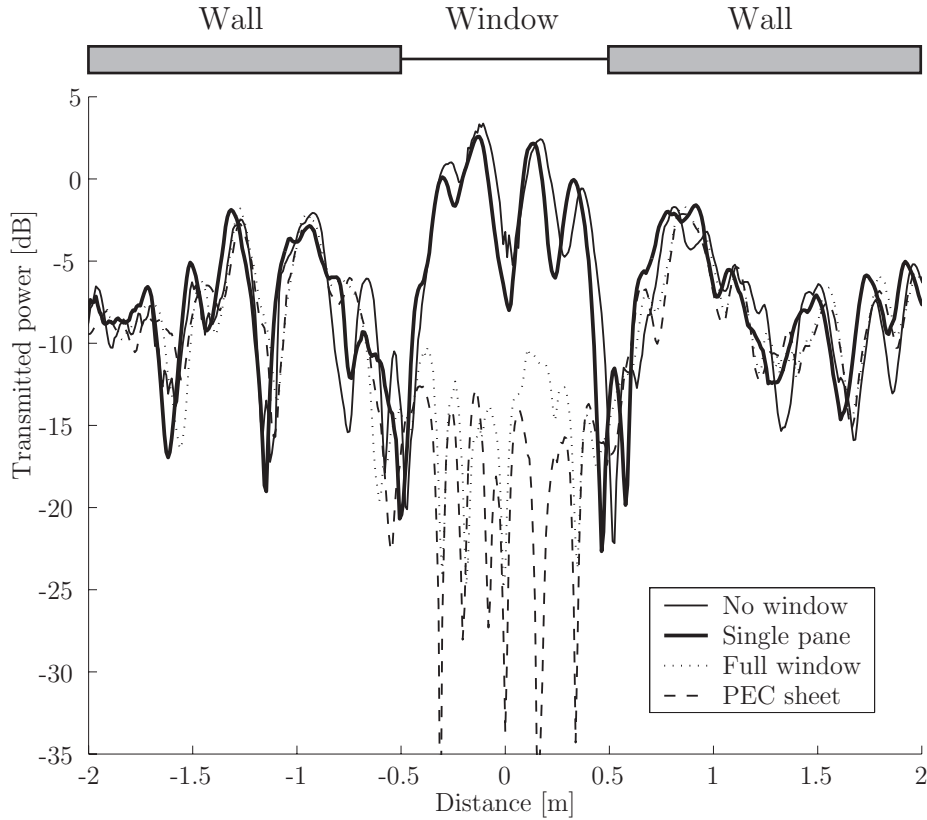
Figure 3: Transmission measurements for different glass plates as a function of the distance along the measurement track, that goes parallel to the window. The four curves are from measurements when (1) no window was fitted in the frame, (2) when a single pane of standard glass was fitted, (3) with a full window consisting of three panes of which one was plated with metal oxide for thermal isolations and (4) with the window replaced by a perfectly conducting (PEC) metal foil. Courtesy of H. Börjesson [2].

Recently, the capabilities of the FSS have been extended by the addition of active devices embedded in the unit cell of the periodic structures. Such structures are also called active grid arrays [18].

3   Mode-matching technique

For the analysis of FSSs several methods can be used, such as the spectral domain approach Galerkin method [3, 9], the mode matching technique [11, 12, 15, 17] or the finite difference time domain approach (FDTD) [1, 6].

In this paper, the mode-matching technique [15] is used for the numerical calculations. The method considers the apertures modelled as short waveguides. The FSS is divided into a number of uniform layers, and the fields in each layer are expanded
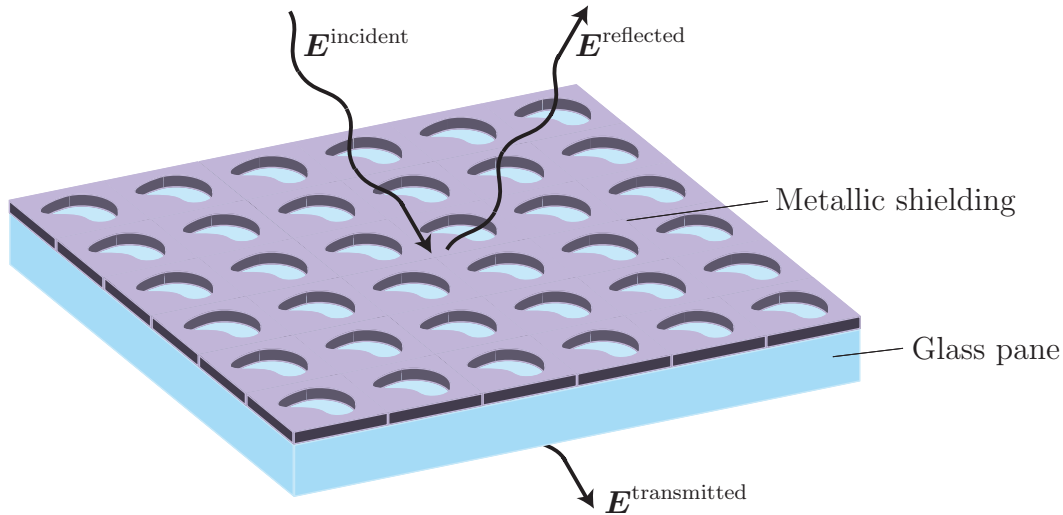
Figure 4: Surface with a periodic pattern of slots.

in a complete set of vector wave functions. The mode matching technique is based on the matching of the total mode fields at each junction to obtain a scattering matrix. The individual scattering matrices are cascade coupled to form an overall scattering matrix for the complete FSS.

The reason that this method was chosen is that it is a general method, where arbitrary structures and arbitrary cross-sections of the apertures can be handled.

3.1 Mode expansion

In Figure 5 a simple FSS, which consists of a perforated conducting plate and a dielectric sheet, is presented. The fields inside the dielectric layers are expanded in tangential plane waves, *i.e.*, Floquet modes, $\boldsymbol{R}_n^{\pm}$, see Figure 5(a). The Floquet modes compose a complete orthogonal set of basis functions. Inside the aperture layers the fields are expanded in waveguide modes $\boldsymbol{E}_p^{\pm}$, which are calculated either analytically or by the Finite Element Method (FEM). The waveguide modes form a complete orthogonal set of basis functions defined on the cross-section of the aperture. The "+"-sign and "-"-sign indicate that the mode propagates in positive and negative direction, respectively.

A plane wave $\boldsymbol{E}^{\mathrm{i}}$ impinges on the FSS in the $\boldsymbol{k}^{\mathrm{i}}$-direction, see Figure 5(a). The scattered field outside the FSS is a discrete sum of plane waves (Floquet waves), where a finite number are propagating waves, while the others are an infinite number of evanescent waves. The scattered field consists of at least two propagating plane waves; the wave $\boldsymbol{E}^{\mathrm{r}}$ propagates in the reflected direction $\boldsymbol{k}^{\mathrm{r}}$, and the wave $\boldsymbol{E}^{\mathrm{t}}$ propagates in the transmitted direction $\boldsymbol{k}^{\mathrm{t}}$.
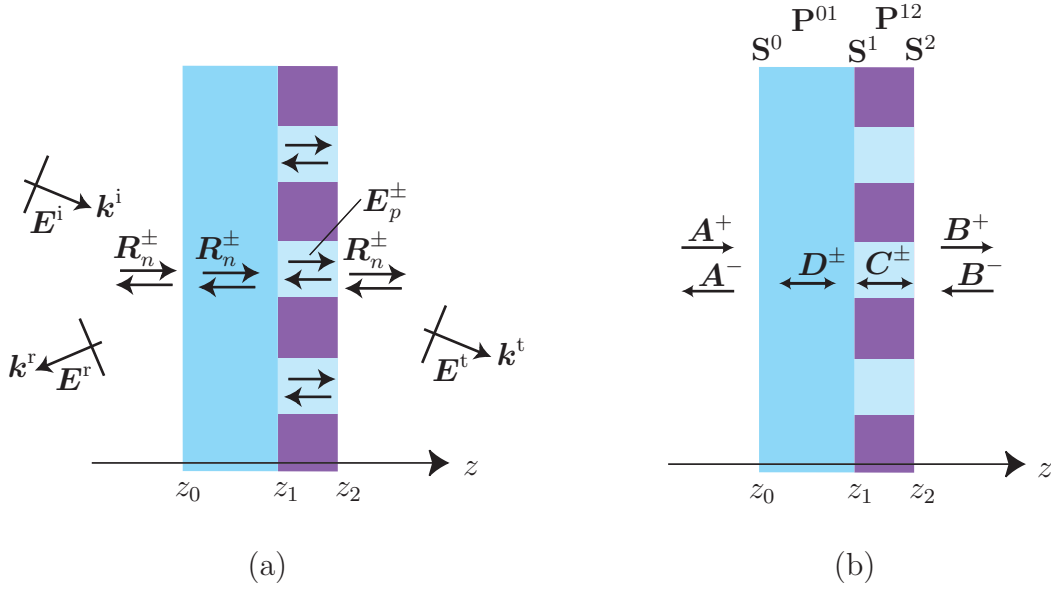
Figure 5: An FSS with two layers; as a model for a glass pane with metallic shielding with slits. (a) The incident field $\boldsymbol{E}^{\mathrm{i}}$, the reflected field $\boldsymbol{E}^{\mathrm{r}}$, the transmitted field $\boldsymbol{E}^{\mathrm{t}}$, the Floquet modes $\boldsymbol{R}_n^{\pm}$, and the waveguide modes $\boldsymbol{E}_p^{\pm}$. (b) The scattering matrices $\mathbf{S}^0, \mathbf{S}^1, \mathbf{S}^2$, the propagation matrices $\mathbf{P}^{01}, \mathbf{P}^{12}$, and the mode coefficients $\boldsymbol{A}^{\pm}, \boldsymbol{B}^{\pm}, \boldsymbol{C}^{\pm}, \boldsymbol{D}^{\pm}$.

3.2 Scattering matrix

The mode-matching technique utilizes the boundary condition to match the tangential electric and magnetic fields at each junction between uniform sections. The boundary conditions say that the tangential electric field is continuous over the entire surface, while the tangential magnetic field is continuous only over the aperture. A linear system of equations is derived from the application of the boundary conditions, relating the mode coefficients at each side of the boundary surface. The relation between the mode coefficients $\boldsymbol{A}^{\pm}, \boldsymbol{B}^{\pm}, \boldsymbol{C}^{\pm}, \boldsymbol{D}^{\pm}$ at each junction is given by a scattering matrix $\mathbf{S}^m$. The amplitudes of the modes can be expressed as the components of the scattering matrix. Each junction along the FSS has its own scattering matrix. For every layer a propagation matrix $\mathbf{P}^n$ is calculated. The scattering matrices for all junctions and the propagation matrices can then be cascaded obtaining an overall scattering matrix $\mathbf{S}$ that describes the scattering properties of the FSS. The scattered and internal fields are known if this scattering matrix and the incident field are known. In Figure 5(b) a scheme of the scattering matrices is presented.

3.3 Numerical calculations

The current method was implemented in MATLAB. The eigenvalue problem for the waveguide modes was solved by FEMLAB [4]. FEMLAB is a commercial FEM pro-
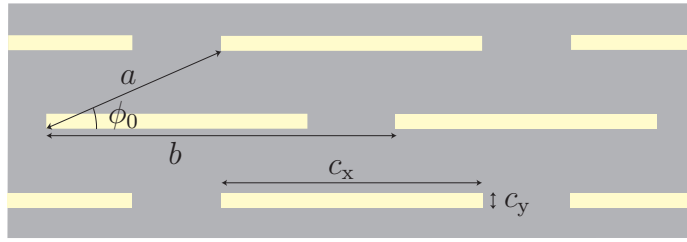
Figure 6: The geometry of the periodic pattern of slits in the metallic shielding.

gram, which can be integrated in MATLAB as a toolbox. In the case of rectangular apertures it is possible to analytically obtain explicit expressions for the modes. However, that was not utilized in this paper.

A substantial number of evanescent modes must be included in the numerical calculations. This is because the uniform sections are usually relatively short in length and thus the amplitude of the decaying modes may still be significant at the next junction. An important question is: How many Floquet modes and waveguide modes are needed? The rule of thumb is that the value of the maximum transverse wavenumber should be the same in all regions to obtain good mode matching.

4 Results

Several simulations of the transmission of microwaves propagating through energy saving window panes with periodic arrays of thin slits in the thin metallic shielding have been performed, *cf.*, Figure 6. A thickness of $18\,\mu$m was chosen for the metallic layer and $4.4\,$mm for the glass. Several values specifying the dimensions of the slits and the periodic pattern were checked in order to obtain a good transmission at $900\,$MHz and $1800\,$MHz. The permittivity of the glass, the angle of incidence and the polarization were varied in order to see the performance of the configuration suggested in this section. The results are given below.

4.1 Optimization

An incident plane wave with horizontal (TE) polarization was assumed as the source of the signal. Normal incidence (angle of incidence $\theta = 0°$) was considered as well as a glass with permittivity $\epsilon_r = 5$. Due to the direction of the slits, a signal with TM-polarization is strongly attenuated, close to $-30\,$dB, when it is transmitted through the window pane, and for this reason TM modes are not considered.

The power transmission for a thin metallic surface is depicted in Figure 7. The length of the slits is chosen to be close to half a wavelength at $900\,$MHz, $c_x = 150\,$mm, and the width to be very narrow, $c_y = 1\,$mm. The periodicity of the pattern is $c_x = 150\,$mm, $c_y = 1\,$mm, $\phi_0 = 45°$. Figure 7 indicates that one can get total transmission through the FSS at a certain frequency by having a periodic array of slits in the metallic shielding. To obtain total transmission at more than one
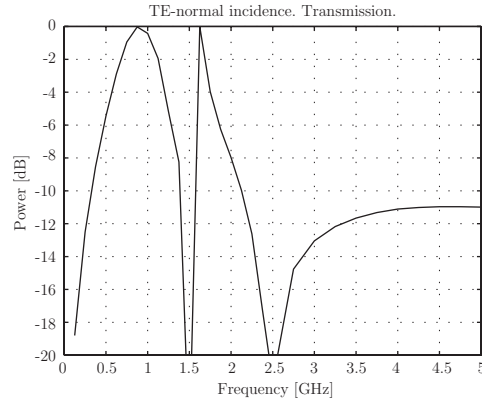
Figure 7: TE normal incidence transmission curve. **Data:** $a = 244\,\mathrm{mm}$, $b = 172.5\,\mathrm{mm}$, $c_x = 150\,\mathrm{mm}$, $c_y = 1\,\mathrm{mm}$, $\phi_0 = 45°$, $\epsilon_r = 5$.
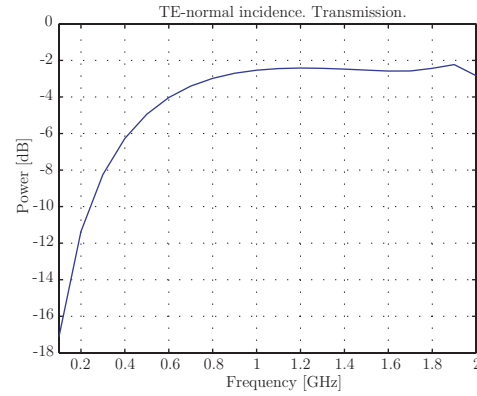
Figure 8: TE normal incidence transmission curve. **Data:** $\phi_0 = 5°$, $\epsilon_r = 5$, $c_x = 190\,\mathrm{mm}$, $a = 215\,\mathrm{mm}$, $b = 172.5\,\mathrm{mm}$.

frequency, or high transmission in a broader frequency band, a more complicated pattern, or structure, is required for the FSS, see *e.g.*, [8, 13, 18].

A large number of geometries and patterns of the slits were tested. From the simulations it was confirmed that the transmission is strongly influenced by the geometry. Small angles of periodicity ϕ_0, see Figure 6, give the best behaviour (flat curve) of the transmission in the frequency band $0 - 2\,\mathrm{GHz}$. Larger values of ϕ_0 give rise to several unwanted dips at certain frequencies. Small deviations (*e.g.*, errors in the manufacturing) from the perfect geometry may move these dips into the frequency band of the radio link. The tests indicate that a value of $\phi_0 = 5°$ is ideal and hence this value was chosen.

The length of the slits, c_x, also has a great influence on the results. In general (depending on the values of a and b), both high and low values result in a faster decrease of the transmission vs. frequency curve around $1800\,\mathrm{MHz}$ and a slower increase around $900\,\mathrm{MHz}$. This is unwanted if high transmission at these two frequencies is desired. A compromise value of $c_x = 190\,\mathrm{mm}$ was chosen as the best in
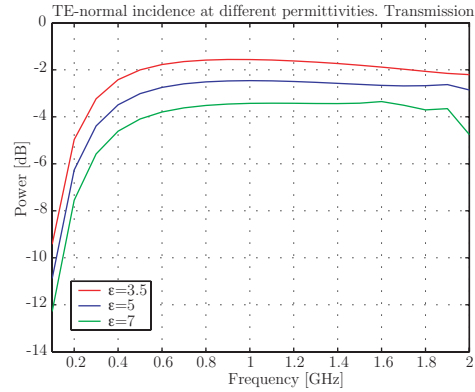
Figure 9: TE normal incidence transmission curve at different permittivities. **Data:** $\phi_0 = 5°$, $\epsilon_r = 3.5, 5, 7$, $c_x = 190\,\text{mm}$, $a = 215\,\text{mm}$, $b = 172.5\,\text{mm}$.

combination with $a = 215\,\text{mm}$ and $b = 172.5\,\text{mm}$. The width of the slits c_y was chosen to 1 mm, in order to remove as little metallic shielding as possible, but letting the power passing through. This geometry gives a number of 224 slits placed in the surface of an $86 \times 84\,\text{cm}$ window. Larger values of a and b imply that less surface is removed from the metallic sheet, but it was observed that this also lower the level of transmission at 900 MHz and/or 1800 MHz. Smaller values of a and b did not give better results.

In Figure 8 the transmitted power through the energy saving window with slits is plotted for frequencies between 0 and 2 GHz. The geometry is given by $\phi_0 = 5°$, $\epsilon_r = 5$, $c_x = 190\,\text{mm}$, $c_y = 1\,\text{mm}$, $a = 215\,\text{mm}$, $b = 172.5\,\text{mm}$. The figure shows a power loss of $-2.7\,\text{dB}$ at 900 MHz and $-2.4\,\text{dB}$ at 1800 MHz, which is an extremely good result considering that the total area of the slits is less than 6% of the area of the window, and considering that, without the slits the attenuation is $-20\,\text{dB}$ at both frequencies [2].

The conclusion is that excellent transmission-frequency curve can be designed by changing the dimensions of the slits and periodicity of the slits, in order to increase or decrease the level of the transmission at the desired frequencies.

4.2 Parameter study

The transmitted power was studied for three different permittivities of the glass, as shown in Figure 9. Depending on the type of window glass plates, the permittivity ϵ_r of the glass ranges between 3.5 and 5 (sometimes up to 7). The transmission levels of the signal decrease with increasing value of ϵ_r. An interesting point is that the flat behaviour of the curve still remains in every case.

Several incident angles were simulated and the corresponding transmission curves are given in Figure 10(a). It can be noted how the desired flat-behaviour obtained at normal incidence is progressively changing into one full of dips at larger angles. The levels of the transmitted signal at 900 MHz and 1800 MHz are affected, especially if the incident angle θ is above $20°$. On account of the signal is composed of several
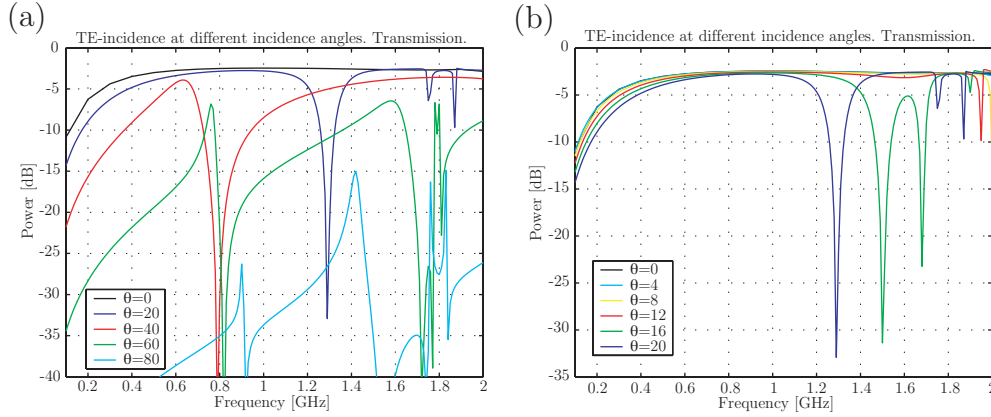
Figure 10: TE incidence transmission curve at different incident angles. (a) $\theta = 0°, 20°, 40°, 60°, 80°$. (b) $\theta = 0°, 4°, 8°, 12°, 16°, 20°$. **Data:** $\epsilon_r = 5$, $\phi_0 = 5°$, $c_x = 190\,\text{mm}$, $a = 215\,\text{mm}$, and $b = 172.5\,\text{mm}$.

multiple reflections, the signal hits the window pane at different angles of incident. Every signal is supposed to have at least one incident angles in the frequency range $0°$ up to $20°$, or in any case if one incident angle is not transmitted anybody else is transmitted. Furthermore, when θ is large, the signal decays as it propagates through the pane, as a result of several reflections. Figure 10(b) focuses on the range of incident angles (0-20°) in which most of the transmission takes place. It shows how some dips appear in the transmitted signal. The dips become more pronounced and move to lower frequencies when the incident angle approaches $20°$. The important feature is that they never affect both the 900 MHz and 1800 MHz frequencies.

The same variation of the incident angle was done for $\epsilon_r = 3.5$, as shown in Figure 11(a). It is observed that a better transmission is obtained at every frequency. Some dips around 1800 MHz disappear, especially the ones that can be observed at $20°$ with $\epsilon_r = 5$. In Figure 11(b) graphs for incident angles between $0°$ and $20°$ are given for panes with $\epsilon_r = 3.5$. Again, there are almost no change of the signal level at 900 MHz and 1800 MHz in this particular range of θ.

4.3   Double glass study

In order to generalize the study, a structure consisting of two panes, one without shielding, and the other with metallic shielding and slits, were analyzed. A width of 47 mm of air was left between the two glasses. In Figure 12(a) results with one and two glasses are presented. Amazingly, at 900 MHz there is a better transmission in the two-glasses case. This can be due to some resonant phenomenon that occurs inside the layers, but this emphasize the possibilities that lie in the slitted metallic shielding technique.

A study of the effect of a variation of the incident angle is shown in Figure 12(c). It can be observed that the dips are moving to lower frequencies as the angle in-
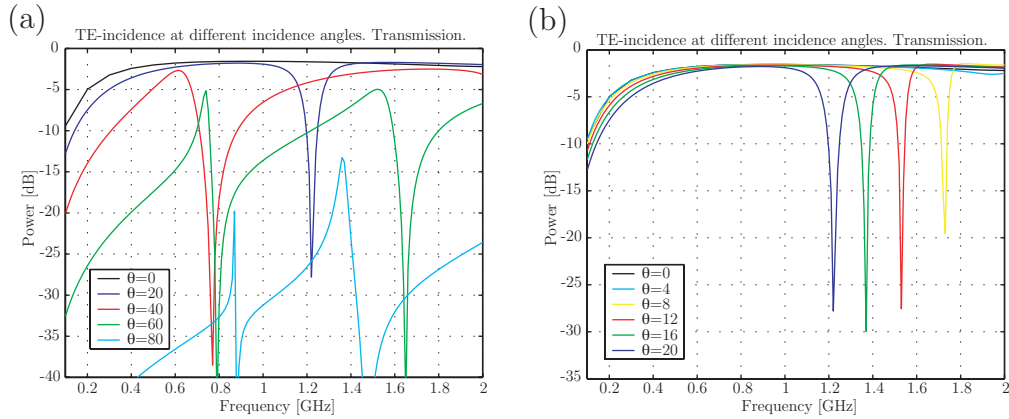
Figure 11: TE incidence transmission curve at different incident angles. (a) $\theta = 0°, 20°, 40°, 60°, 80°$. (b) $\theta = 0°, 4°, 8°, 12°, 16°, 20°$. **Data:** $\phi_0 = 5°$, $\epsilon_r = 3.5$, $c_x = 190\,\text{mm}$, $a = 215\,\text{mm}$, and $b = 172.5\,\text{mm}$.

creases. There is an undesired one at 900 MHz when $\theta = 40°$, but a good behaviour can be noted up to $\theta = 10°$.

Finally, the ϵ_r of both glasses was changed, as can be observed in Figure 12(b). The influence of the ordering of the panes with different ϵ_r is depicted, and as seen from the graphs the best result is obtained if the first pane that the wave reaches is the one with $\epsilon_r = 3.5$.

5   Conclusions

A technique that gives an excellent improvement of the transmission through energy saving window panes at 900 MHz and 1800 MHz has been presented. The technique utilizes an array of very narrow slits in the shielding surface. It has also been shown how the transmission through the window depends on the angle of incidence, permittivity of the glass, and if single or double glass is used. With the suggested optimized slit geometry, good transmission results at both of the above mentioned frequencies were obtained.
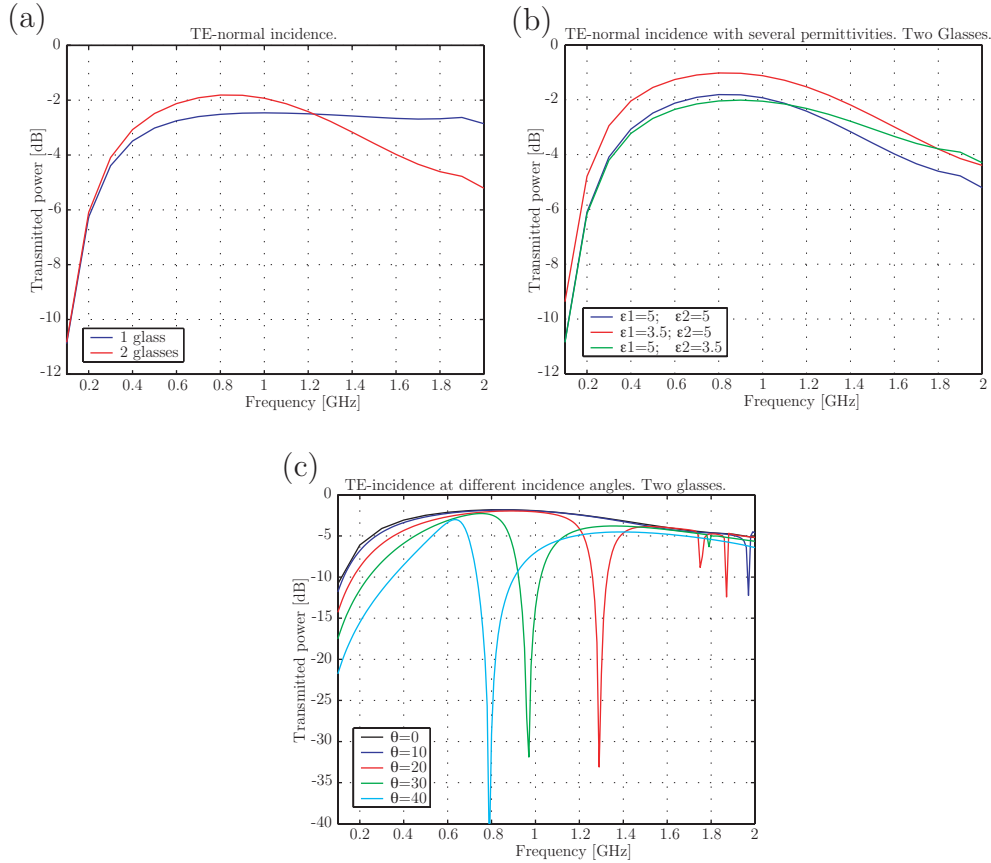
6   Acknowledgments

(a)

(b)

(c)

Figure 12: (a) TE normal incidence transmission curve for one and two panes. $\epsilon_{1,2} = 5$. (b) TE normal incidence transmission curve for different permittivities for two panes; $\epsilon_1, \epsilon_2 = 3.5, 5$. (c) TE incidence transmission curve for different incident angles for two panes; $\theta = 0°, 10°, 20°, 30°, 40°$. In all three graphs: $\phi_0 = 5°$, $c_{\mathrm{x}} = 190\,\mathrm{mm}$, $a = 215\,\mathrm{mm}$, and $b = 172.5\,\mathrm{mm}$.

References

[1] A. Boag and R. Mittra. A numerical absorbing boundary-condition for finite-difference and finite-element analysis of open periodic structures. *IEEE Trans. Microwave Theory Tech.*, **43**(1), 150–154, 1995.

[2] H. Börjesson. *Radio Wave Propagation in Confined Environments.* PhD thesis, Lund Institute of Technology, Department of Applied Electronics, P.O. Box 118, S-221 00 Lund, Sweden, 2000.

[3] C. H. Chan and R. Mittra. On the analysis of frequency-selective surfaces using subdomain basis functions. *IEEE Trans. Antennas Propagat.*, **38**(1), 40–50, 1990.

[4] COMSOL AB, Stockholm, Sweden. *FEMLAB: Reference Manual*, 2000.

[5] D. C. Cox, R. R. Murray, and A. W. Norris. 800 MHz attenuation measured in and around sub-urban houses. *AT & T Bell Laboratories Technical Journal*, **63**(6), Jul.–Aug. 1984.

[6] P. Harms, R. Mittra, and W. Ko. Implementation of the periodic boundary-condition in the finite-difference time-domain algorithm for FSS structures. *IEEE Trans. Antennas Propagat.*, **42**(9), 1317–1324, 1994.

[7] D. Molkdar. Review on radio propagation into and within buildings. *IEE Proceedings-H*, **138**(1), 61–73, 1991.

[8] B. Munk. *Frequency Selective Surfaces: Theory and Design*. John Wiley & Sons, New York, 2000.

[9] S. Poulsen. Scattering from frequency selective surfaces: A continuity condition for entire domain basis functions and an improved set of basis functions for crossed dipole. *IEE Proc.-H Microwaves, Antennas and Propagation*, **146**(3), 234–240, 1999.

[10] T. S. Rappaport and S. Sandhu. Radio-wave propagation for emerging wireless personal communication systems. *IEEE Antennas and Propagation Magazine*, **36**(5), 14–24, October 1994.

[11] A. Roberts. *Modal methods for gratings, grids and apertures*. PhD thesis, School of Physics, University of Sydney, 1988.

[12] A. Roberts and R. C. McPhedran. Bandpass grids with annular apertures. *IEEE Trans. Antennas Propagat.*, **36**(5), 607–611, May 1988.

[13] J. C. Vardaxoglou. *Frequency Selective Surfaces (Analysis and Design)*. Research Studies Press, 1997.

[14] E. H. Walker. Penetration of radio signals into buildings in the cellular radio environment. *The Bell System Technical Journal*, **62**(9), November 1983.

[15] B. Widenberg. A general mode matching technique applied to bandpass radomes. Technical Report LUTEDX/(TEAT-7098)/1–33/(2001), Lund Institute of Technology, Department of Electroscience, P.O. Box 118, S-221 00 Lund, Sweden, 2001.

[16] B. Widenberg, S. Poulsen, and A. Karlsson. The design of windowpanes with high transmission at 900 MHz and 1800 MHz. In *Antenn 00, Nordic Antenna Symposium, Lund, Sweden*, pages 185–190, 2000.

[17] B. Widenberg, S. Poulsen, and A. Karlsson. Scattering from thick frequency selective screens. *J. Electro. Waves Applic.*, **14**(9), 1303–1328, 2000.

[18] T. K. Wu, editor. *Frequency Selective Surface and Grid Array*. John Wiley & Sons, New York, 1995.

[19] T. K. Wu and S. W. Lee. Multiband frequency-selective surface with multiring patch elements. *IEEE Trans. Antennas Propagat.*, **42**(11), 1484–1490, 1994.